Nanoscale

eHigh-Performance Graphene/Sulphur Electrodes for Flexible Li-Ion Batteries Using Low-Temperature Spraying Method

Pushpendra Kumar[1,2], Feng-Yu Wu[3], Lung-Hao Hu[4], Sayed Ali Abbas[2], Jun Ming[3], Chia-Nan Lin[5], Jason Fang[5], Chih-Wei Chu[2*], Lain-Jong Li[3*]

[1]Department of Electrophysics, National Chiao Tung University, Hsinchu 300, Taiwan.

[2]Research Center for Applied Science, Academia Sinica, Taipei 11529, Taiwan.

[3]Physical Science and Engineering Division, King Abdullah University of Science & Technology (KAUST), Thuwal 23955, Saudi Arabia.

[4]Southern Taiwan University of Science and Technology, Tainan, 710, Taiwan.

[5]Material and Chemical Research Laboratories, Industrial Technology Research Institute, Hsinchu, 31040, Taiwan

*To whom correspondence should be addressed: gchu@gate.sinica.edu.tw and

lance.li@kaust.edu.sa

Abstract

Elementary Sulphur (S) has been shown as an excellent cathode material in energy storage devices such as Li-S batteries owing to its very high capacity. The major challenges associated with the sulphur cathodes are structural degradation, poor cycle performance and instability of the solid-electrolyte interphase caused by the dissolution of polysulfides during cycling. Tremendous efforts by others have demonstrated that encapsulation of S materials improves their cycle performance. To make this approach practical for large scale application, the use of low-cost technology and materials has become a crucial and new focus of S-based Li-ion batteries. Herein, we propose to use a low temperature spraying process to fabricate graphene/S electrode material, where the ink is composed of graphene

flakes and the micron-sized S particles prepared by grinding of low-cost S powders. The S particles are found to be well hosted by highly conductive graphene flakes and consequently superior cyclability (~70% capacity retention after 250 cycles, good coulombic efficiency (~98%) and high capacity (~1500mAh/g) are obtained. The proposed approach does not require high temperature annealing or baking; hence, another great advantage is to make flexible Li-ion batteries. We have also demonstrated two types of flexible batteries using the sprayed graphene/S electrodes.

Introduction

The demand for the next generation high-capacity energy-storage materials is essential because high-performance energy storage and renewable power generationdevices will be hard to achieve without these materials. Rechargeable Li ion batteries have become very promising energy storage devices for the emergent need in sustainable and clean energy applications due to their high specific energy and reasonable cost [1-10]. Huge efforts have been devoted to lithium-sulphur batteries since they can offer a higher capacity than currently used active materials [11−15]. The theoretical limit of specific capacity for the sulphur cathode is nearly 1675mAh/g or its specific energy of ~2600 Wh/kg that is considerably advanced than the conventional lithium ion batteries. The configuration of Li-S battery cell simply consists of sulphur as the positive electrode and lithium as the negative electrode [16-18]. A Li-S battery differs from the conventional Li-ion batteries based on metal oxide cathodes, where the batteries operate on the basis of intercalation/deintercalation processor reversible uptake of Li ions and electron using the active oxides. The storage mechanism of Li-S cell is governed by the chemical reaction: during discharge, the cathode undergoes formation of several intermediate soluble polysulphide species like Li_2S_8, Li_2S_6 and Li_2S_4) and ends up with the formation of solid Li_2S_2 and Li_2S. On the other hand, Li_2S_2

and Li$_2$S may transform to S again via same soluble polysulphide intermediates during the charging. [19]

Despite of its high capacity, there are prime challenges associated with S cathodes such as insulating nature of S, structural degradation, poor cycle performance and instability of the solid-electrolyte interphase during cycling. Poor cyclability and instability in the system is primarily because of the high solubility of the polysulphide anions formed as reaction intermediates during lithiation/delithiation processes in the presence of electrolytes [20]. During cycling process, the intermediate anions of polysulphide migrate through the separator towards Li electrode as a result of which they are reduced to solid precipitates (Li$_2$S$_2$ and/or Li$_2$S), causing the loss of active mass [21].

Many approaches have been adopted to settle this issue. Nazar et al. have used mesoporous carbon to encapsulate sulphur and attained a high specific capacity at around 1300 mAh/g [22, 23]. Diverse carbon nanostructures have also been progressively reported to enhance the electrochemical performance of Li-S cells including hollow/porous carbon spheres [24, 25] hollow carbon nanofibers [26, 27] activated carbon fibres [28] and graphene oxides [29,30]. In addition to carbon materials, oxides additives such as mesoporous silica [31] TiO$_2$ [32] and metal-organic framework (MOF) [33] also help to enhance the performance of the sulphur cathodes. Moreover, polymer modified sulphur electrode also exhibits good cycling performance [22, 30, 34]. All these advances help to build up the confidence and knowledge of using S as the high capacity electrodes for emerging applications.

Graphene is another type of carbon material which exhibits high conductivity and it has been demonstrated as an additive or encapsulating agent to enhance the battery performance either for conventional LiFePO$_4$ [35-36] or S cathodes [11-19, 37]. Meanwhile, high energy density of rechargeable batteries has transformed their shape and size to serve for portable,

printed and wearable electronics. Graphene is considered as the promising material for the development of flexible batteries. In this article, we propose a simple and scalable spraying process to fabricate high capacity S-based electrodes, where the ground S particles and thin graphene flakes were used to formulate the ink solution for spraying. Results show that the S particles are well enveloped by highly conductive graphene bundles and S particles have enough room for volume expansion and contraction during lithiation/delithiation process. Consequently, the solid-electrolyte interphase remains stable and spatially confined, resulting in superior capacity and cyclability. Since the 2nd function of graphene flakes is to enhance the conductivity of the electrodes, no extra conductive carbon materials are needed. The proposed approach only requires gentle heating (80 ^{o}C) on substrates for spraying and no high temperature annealing or baking is needed. Hence, our proposed electrode process is to serve for flexible Li-ion batteries. Two prototypes of flexible batteries based on our sprayed graphene/S electrodes have been demonstrated workable in this contribution.

Experimental Section:

Graphene Sheets

The graphene flakes (provided by Nitronix Nanotechnology Inc. Taiwan) were prepared by a scalable method modified from the reported electrochemical exfoliation [38]. Figure 1a shows the atomic force microscopy (AFM) image for the as-received graphene flake casted on a Si substrate. The lateral size of these graphene sheets ranges from 10 to 30 micron observed from an optical microscope. The thickness of the graphene flakes is from 4 nm to 15 nm, obtained by statistical AFM measurements (Supporting Figure S1). Selected Raman and X-ray photoemission spectroscopy (XPS) results for these flakes are also shown. For comparison, another type of commercially available graphene sheet, reduced graphene oxide (r-GO), was purchased from Sigma Aldrich and directly used in our experiments.

Grinding of Sulphur Powders

The bulk S powders were ground in a liquid media with the help of high energy miller using micron-sized silica balls. The commercially available sulphur powders (3.0 g; from Sigma Aldrich) and 160 ml of isopropyl alcohol were put in the grinding chamber along with 50 µm zirconia dioxide beads (600 g) for grinding. The grinding was performed at 2000 rpm for 6 hours at room temperature. Figure 1b displays the scanning electron microscopy (SEM) image for the ground S powders, where the size of obtained S particles is reduced to around a few microns and they become dispersible in the solvent N-Methyl-2-pyrrolidone (NMP).

Preparation of Graphene/Sulphur Composition by Spraying

For the present investigation, the graphene flakes were dispersed in NMP (0.2 g in 20 ml) with the aid of ultrasonication (water bath) for 90 mins before it is mixed with ground S particles. To prepare a precursor ink for spraying, the polyvinylidenedifluoride (PVDF) binder (20wt% of the total solid content) is also added. Taking the composition graphene: S = 20:80 weight ratio as the example, 0.8 g of micron-sized S particles and 0.20g of PVDF binder were added in above graphene (0.2 g) dispersion in NMP and the mixture was ultrasonicated for another 180 min. This mixture was then sprayed directly onto an Al current collector with the help of a spray nozzle using N_2/Ar as a carrier gas while keeping the Al foil at 80 ^{o}C, as illustrated in Figure 1c. After spraying, the sample was dried at 60 ^{o}C for 2-6 hrs in a vacuum oven. For all the graphene/S electrodes (10:90, 20:80 and 30:70) were prepared in this study, they contained the same percentage of binder (20 wt% of the total solid content).

Electrochemical Characterization

CR2032 coin-type half-cells were assembled in an Ar-filled glove box. 1.0 M lithium bis(trifluoromethanesulfonyl) imide in 1,3-dioxolane (DOL) and 1,2-dimethoxyethane (DME) (1:1 = v/v) containing 1 wt% $LiNO_3$ was used as the electrolyte. The cells were assembled by sandwiching separators (polypropylene, Celgard 2325) with the working electrodes and lithium metal (Reference/counter electrode). The cells were electrochemically cycled between 1.5 and 3 V versus Li^+/Li at different current densities under constant current mode for both charge and discharge cycles.

Fabrication of Flexible Batteries

With the low temperature spraying process developed here, we fabricate two types of flexible batteries. (1)The as-sprayed graphene/S composite serves as the cathode and Li metal foil is the counter electrode. The separator is 20 μm microporous tri-layer membrane (PP/PE/PP) Celgard 2320 (from Celgard, LLC Corp., USA). An organic electrolyte is prepared by dissolving 1.0 M $LiN(CF_3SO_2)_2$ and 0.2 M $LiNO_3$ in a mixture of 1,2-dimethoxyethane (DME) and 1,3-dioxolane (DOL) mixed in a 1:1 volumetric ratio. Nylon and aluminium films (from Dai Nippon Printing Co., Ltd.) are used as packing covers for the flexible battery.(2) The conventional $LiMn_2O_4$ is used as the cathode and as-sprayed graphene/S is the anode. The separator is the tri-layer membrane (PP/PE/PP).The electrolyte is prepared by dissolving 1 M Lithium bis (trifluoromethanesulfonyl) imide (LiTFSI) in a mixture of DME (dimethyl ether) and DOL (1, 3-dioxolane) with the ratio 2:1 (v/v), where 1wt% $LiNO_3$ is also added. Aluminium laminate multi-layered polypropylene film is used as the packing material.

Spectroscopic Characterizations:

Surface morphology characterization (top and cross-section view) and energy dispersive X-ray (EDS) elemental mapping analysis were carried on in a FEI Nova 200 SEM system. The topological studies of graphene sheets were performed in a Bruker Dimension-Icon AFM system. For the AFM characterization, the graphene dispersed in ethanol was drop-cast on a SiO_2 substrate.

Results and discussion

The major objective of the present research is to obtain a highly stable and high-capacitance graphene/S composite to serve as an electrode for flexible Li ion batteries. Air-spraying is attractive since it is a scalable, low-cost and low-temperature compatible process for making electrodes. The hydrothermal or chemical processes to synthesize S particles for Li-S batteries have been proposed [39]. In order to make the preparation of graphene/S ink as simple and scalable as possible, we use the cheap commercial S powders as the sulphur source. To spray the graphene/S ink solution and avoid the clogging at the spraying nozzle, purchased S powders need to be ground to have a proper particle size. The downscaled size also ensures the increase in active surface areas. The simple spraying technique of electrode fabrication introduces several obvious advantages: (1) The composition of graphene/S electrode is pre-determined by the composition of the precursor solution. (2) The spraying process can be performed at a low temperature (80 $^\circ$C in our experiments) and no high temperature annealing or baking process is needed in the electrode preparation process; hence, the method is compatible with flexible electronics. This feature may potentially serve for the electrodes in versatile applications, such as printed electronics (i.e., touch-panel) and flexible electronics (i.e., solar cell, organic light-emitters). (3) The thickness of the sprayed materials can be easily controlled by the amounts of the materials sprayed, and the size of the electrode is also not limited. These are critically important for the controllable and scalable processes. In our experiments, the typical thickness of the graphene/S material is

around ~45 μm thick (Supporting Figure S2). Another very unique feature of our batteries is that the frequently used conductive carbon additive is not necessary since graphene flakes themselves can promote the conductivity of the electrode.

To examine the electrical properties of the sprayed graphene/S electrodes, coin-type CR2032 half-cells were assembled, where the graphene/S is used as a cathode and Li metal is the anode as described in the experimental section. Figure 2a shows the 1st cycle Galvanostatic charge/discharge profiles of the graphene/S cells at a current density of 50mA/g with a potential window of 1.5–3.0 V versus Li^+ /Li^0, where we compare the performance for three compositions (graphene : S weight ratio = 30:70, 20:80 and 10:90). To reveal the effect of a graphene capping layer on graphene/S, we have also prepared the 20:80 electrodes with an extra graphene capping layer, where the capping layer (~20 μm thick) was also prepared by the spaying method using the ink containing only graphene flakes. All the discharge profiles are composed of two plateaus, which have been identified as the reduction of elemental sulfur (S_8) to long chain lithium polysulfides at a higher voltage (>2.25V) and the formation of short-chain Li_2S_2/Li_2S at a lower voltage (2.05 – 2.1 V) [40-41]. Note that all the specific capacity is calculated based on the actual weight of sulphur in the electrodes. The initial discharge specific capacity of the sample (10:90) is ~1340 mAh/g and the capacity for the samples (20:80) and (30:70) is similar ~1400 mAh/g. It is noted that the sample (20:80) with a graphene capping layer shows the highest capacity~1500 mAh/g. Figure 2b displays the 2nd cycle charge/discharge profiles for these electrodes, where we observe that the capacity of the sample (10:90) drastically decreases to ~1040 mAh/g, indicating that the 10% graphene is not enough to secure or protect the S particles. The samples (20:80) and (30:70) remain their capacity at a value higher than 1200 mAh/g. The best performance still goes to the sample (20:80) with a capping layer. It seems that the overall performance of the electrodes is determined by the composition. If the

sulphur content is too high, the graphene cannot provide enough protection to S dissolution in electrolyte. Dissolution of S in the electrolyte leads to the formation Li sulphides in electrolytes, which is believed to be the foremost reason for shuttling effect and rapid capacity fade in Li–S batteries. On the other hand, if the sulphur content is too low, it is suggested that the formation of polysulfides during the charge process will be easier to dissolve in the electrolyte, leading to the shuttling phenomenon [42]. So, lower S content is not favourable since the overall capacity per electrode weight is lower. As a control, Graphene-S composite was prepared by simple mechanical mixing with the ratio Graphene: S = 20:80. The charge/discharge performance and cycling test under the same current density are presented in Supporting Figure S3. Due to the non-homogenous distribution of Graphene and S through the mechanical mixing, the specific capacity faded quickly.

Since the experimental results suggest that ratio (20:80) leads to better capacity retention, we performed the rate performance measurement for the samples (20:80) with and without capping at different current densities as indicated in Figure 2c. With the cycling at 50, 100, 200, 400, 800, 1600 mA/g, the (20:80) sample without capping shows reversible discharge capacities of around 1390, 1180, 959, 623 and 468 mAh/g respectively. The electrode ((20:80) + capping) consistently shows higher discharge capacities of around 1500, 1320, 1150, 750 and 500 mAh/g respectively. Figure 2d displays the cycling stability of these two samples at thecharge/discharge rate of 100mA/g for more than 250 cycles. The average coulombic efficiency is about 98% for the tested samples (Supporting Figure S4). In general, the structure with a capping layer performs better in the first 100 cycles, where its capacity is significantly higher than the sample without capping. Nevertheless, at 200 cycles, the capacity maintains at 760 mAh/g, which is closer to the 700 mAh/g for the uncapped sample. The results in Figures 2a-2c suggest that the capping layer is able to efficiently suppress the S dissolution from electrodes to the electrolytes in the beginning. After a large

number of electrochemical cycles, the rate capability is still dominated by the initial graphene:S composition, which is likely related to the morphology of the sprayed graphene/S electrodes.

Figure 3a and 3b show the angle-tiled SEM images of the surfaces of the sample (20:80), where the layered graphene structures and particle-shaped S are observed. The graphene sheets possess highly porous interconnected structure. It could therefore serve as a porous network that can host S particles and provide mechanical support and electrically conductivity. Figure 3c shows the cross-sectional view of the (20:80) electrode, where the distribution of C and S elements obtained from EDS elemental mapping for the indicated area demonstrates that C and S are mixed in a homogenous manner. Supporting Figure S5 shows the top view SEM images and related EDS mapping of the sprayed graphene-S composite after cycling (sample graphene-S=20:80). The results confirm the uniform distribution of S even after cycling. TEM images in supporting Figure S6 clearly reveals the highly crystalline nature of graphene in the graphene/S mixture. From high-resolution TEM images it is also confirmed that the graphene remains its few-layered structure without obvious aggregation.

For comparison, the commercially available r-GO flakes are also adopted to prepare electrodes. The same composition of graphene/S (20:80) electrode exhibits a specific 1st cycle discharge capacity as high as 1650 mAh/g as shown in Figure 4. The SEM image and EDS element mapping in Figure 4b inset also prove that the graphene and S are distributed homogeneously across the sample. However, the charge/discharge curves reveal a polarization effect which is unfavorable for battery application. It has been suggested that the high polarization in Li-S cell is generally due to the non-conductive nature of Li_2S_2 and Li_2S [43].The actual underlying mechanism requires more studies.

As the demonstration of the sprayed graphene/S electrodes, we fabricate two types of flexible Li-ion batteries. Figure 5a shows that the flexible battery using commercial $LiMn_2O_4$ as the cathode and the sprayed graphene/S (20:80) as the anode, where the voltage output was about 1.95 V and the power output is able to light up a red LED under a folded situation. On the other hand, the graphene/S (20:80) electrode can be used as a cathode and a Li metal as the anode. Figure 5b demonstrates the voltage from this type of batteries is 3.05 V. The output 3.05 V in Fig. 5b is the initial open-circuit voltage (OCV) of lithium sulfur battery which could shift to its theoretic value of ~ 2.4 to 2.5 V and the adjacent image represent lighting up a green LED under bended condition.

Conclusions

A simple and scalable spraying process to fabricate graphene/Sulphur electrodes is reported, where the ink is composed of ground sulphur micro-particles and graphene flakes. Both materials are considered as low-cost materials. Superior cyclability (nearly 70% capacity retention after 250 cycles) and high capacity (~1500 mAh/g) are obtained. The fabrication of the electrodes does not require extra carbon additives and it can be performed at a low temperature ($<80^{o}C$). Two prototypes of flexible batteries based on the sprayed electrodes have been demonstrated. This research may encourage the advancement of scalable production of high-performance and next-generation batteries based on S active materials.
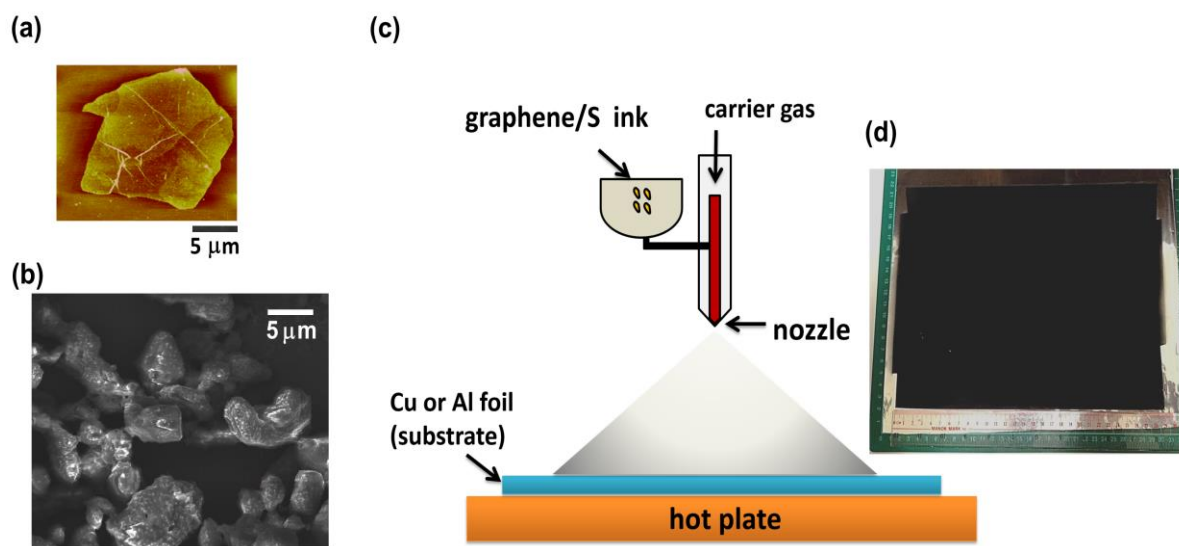
Acknowledgements

Figures:

Figure 1. (a) AFM image of the graphene flake drop-cast on a SiO$_2$/Si substrate. (b) Scanning electron microscopic image for the ground S powders. (c) Schematic illustration for the spraying process. (d) Photo of the sprayed graphene/S electrode.
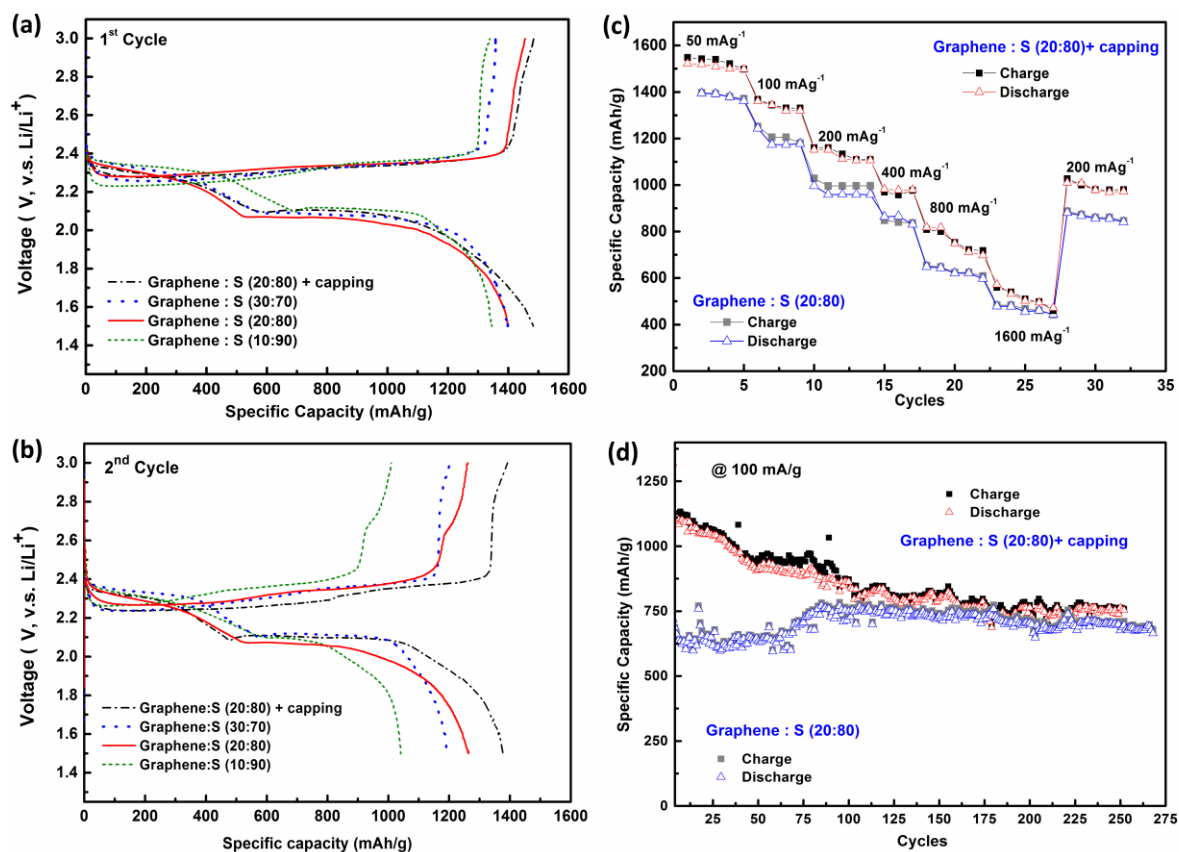
Figure 2. (a)1st cycle and (b) 2nd cycle Galvanostatic charge/discharge profiles of the graphene/S cells at a current density of 50mA/g with a potential window of 1.5–3.0 V versus Li^+/Li^0. (c) The rate performance measurement for the samples (20:80) with and without capping at different current densities. (d) The cycling stability of thetwo samples (20:80) with and without capping at the charge/discharge rate of 100mA/g for more than 250 cycles.
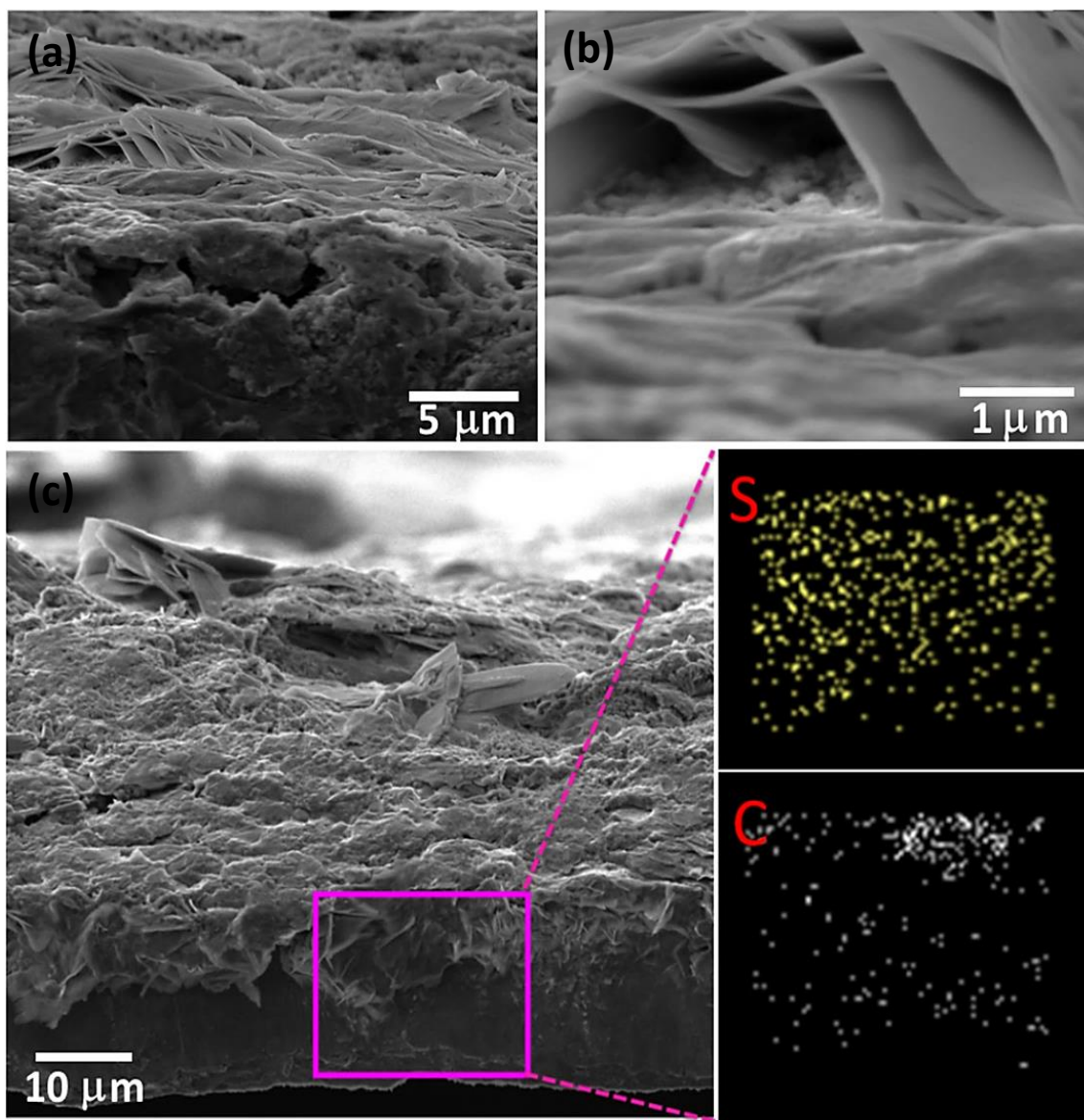
Figure 3. (a,b)The tilt-angled SEM images of the surfaces of the sample (20:80), where the layered graphene structures and S particles are observed.(c) The cross-sectional view of the graphene: S electorde (20:80). The distribution of C and S elements from EDS elemental mapping are also shown.
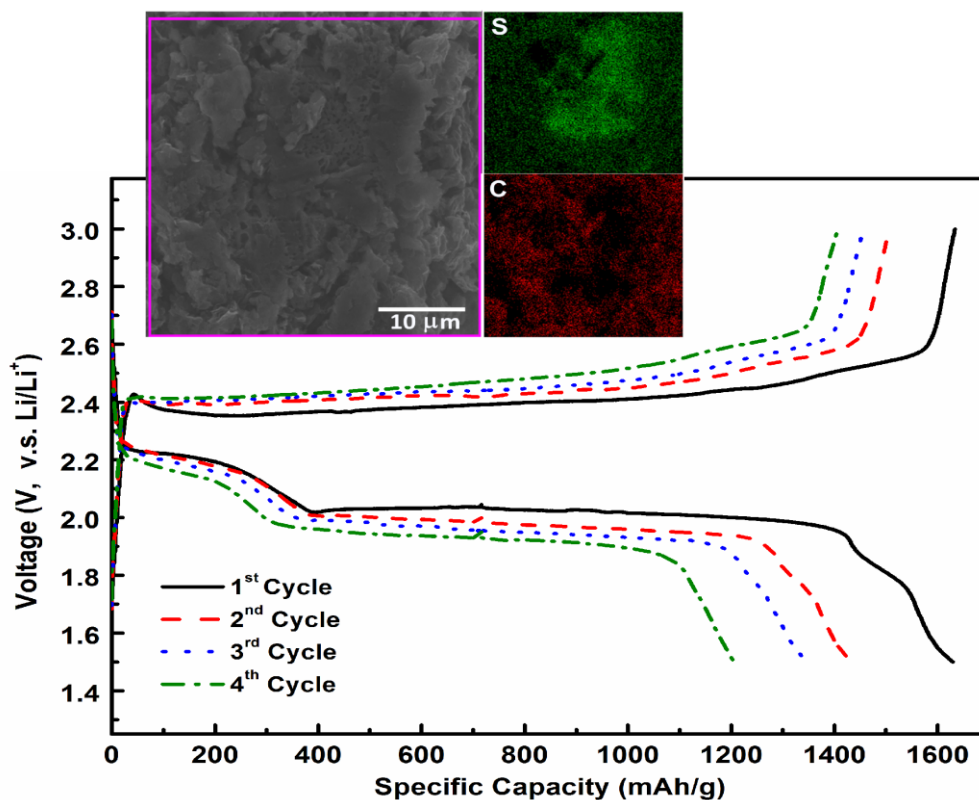
Figure 4. Galvanostatic charge/discharge profiles of the cell based on r-GO/S electrode, where the composition is r-GO:S = 20:80 at a current density of 50mA/g with a potential window of 1.5–3.0 V versus Li^+/Li^0. Inset shows the SEM images andEDSelement mapping for C and S.
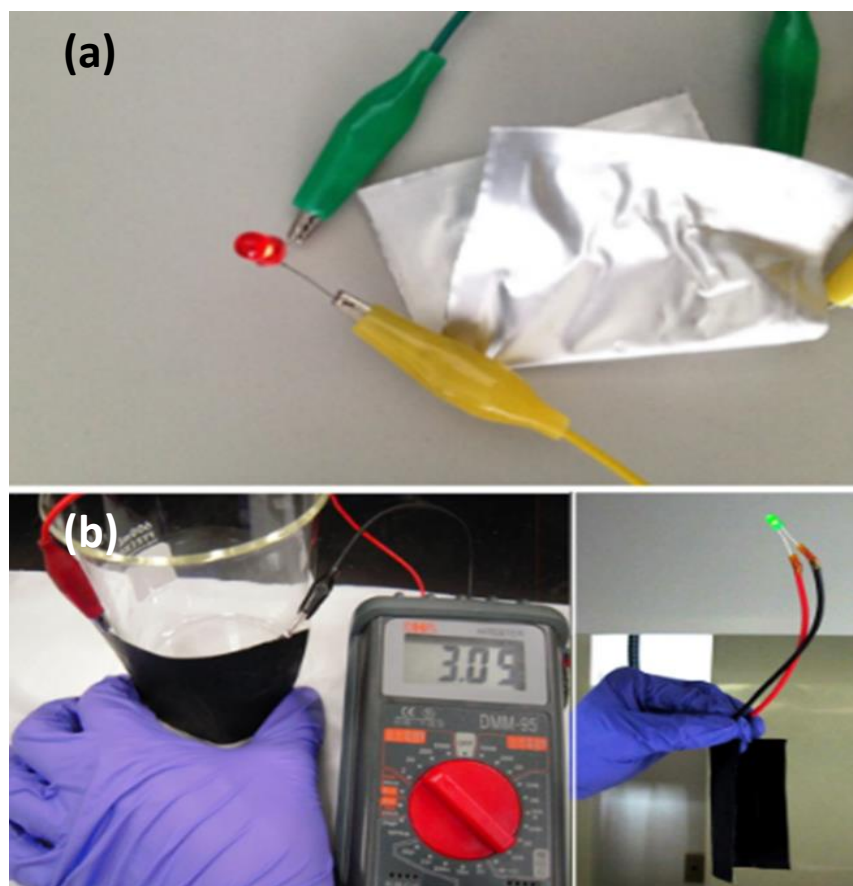
Figure 5. (a)The flexible battery using commercial LiMn$_2$O$_4$ as the cathode and the sprayed graphene/S (20:80) as the anode. The voltage output from the battery is around ~1.95 V. (b) The flexible battery using graphene/S (20:80) electrode as the cathode and the Li metal as the anode. The voltage output from this type of batteries is 3.05V. The voltage 3.05 V in Fig. 5b is the initial open-circuit voltage of lithium sulfur battery of graphene-S/Li, which shifts to its theoretical value ~ 2.4 to 2.5V at a later stage.

References:

1 M. Winter and R. Brodd, *Chem. Rev.* 2004, **104**, 4245-4269.

2 P. G. Bruce, *Solid State Ion.* 2008, **179,** 752-760.

3 (**a**) D. Yang, Z. Lu, X. Rui, X. Huang, H. Li, J. Zhu, W. Zhang, Y. M. Lam, H. H. Hng, H. Zhang and Q. Yan, *Angew. Chem. Int. Ed.* 2014, **53,** 9352-9355. (**b**) C. Guan, X. Li, H. Yu, L. Mao, L. H. Wong, Q. Yan and J. Wang, *Nanoscale***,** 2014, **6**, 13824-13830. (**c**) X. Huang, H. Yu, H. Tan, J. Zhu, W. Zhang, C. Wang, J. Zhang, Y. Wang, Y. Lv, Z. Zeng, D. Liu, J. Ding, Q. Zhang, M. Srinivasan, P. M. Ajayan, H. H. Hng and Qingyu Yan, *Adv. Funct. Mater.* 2014, **24,** 6516-6523. (**d**) Y. Tang, Y. Zhang, J. Deng, D. Qi, W.R. Leow, J. Wei, S. Yin, Z. Dong, Z. Chen and X. Chen, *Angew. Chem. Int. Ed.* 2014, **53**, 13488. (**e**) Y. Tang, X. Rui, Y. Zhang, T.M. Lim, Z. Dong, H. H. Hng, X. Chen, Q. Yan and Z. Chen, *J. Mater. Chem. A*, 2013, **1**, 82-88. (**f**) Y. Tang, Y. Zhang, J. Deng, J. Wei, H. L. Tam, B. K. Chandran, Z. Dong, Z. Chen and X. Chen, *Adv. Mater.* 2014, **26**, 6111-6118.

4 (**a**) Y. Zhou, D. Yang , Y. Zeng, Y. Zhou, W. J. Ng, Q. Yan and E. Fong, *Small*, 2014, **15**, 3997-4002. (**b**) L. Lai, J. Zhu, B. Li, Y. Zhen, Z. Shen, Q. Yan and J. Lin, *Electrochimica Acta***,** 2014, **134,** 28-34. (**c**) J. Zhu, D. Yang, Z. Yin, Qingyu Yan and Hua Zhang, *Small,* 2014, **10,** 3480-3498.

5 (**a**) X. Rui, Q. Yan, T. M. Lim and M. S-Kazacos, *J. Power Sources***,** 2014, **258** 19-38. (**b**) L. Lai, J. Zhu, Z. Li, D. Y. W. Yu, S. Jiang, M. Subodh, Q. Yan, Y. M. Lam, Z. Shen, and L. Jianyi, *Nano Energy*, 2014, **3** 134-143.

(**c**) X. Zhou, G. Wu, J. Wu, H. Yang, J. Wang, G. Gao, R. Cai and Q. Yan, *J. Mater. Chem. A,* 2013, *1,* 15459-15468.

6 (**a**) J. Zhu, D. Yang, X. Rui, D. Sim, H. Yu, H. E. Hoster, P. M. Ajayan and Q. Yan, *Small*, 2013, **9,** 3390-3397. (**b**) X. Cao, Y. Shi, W. Shi, X. Rui, J. Kong, Q. Yan and H. Zhang, *Small***,** 2013, **9,** 1703-1707. (**c**) J. Zhu, Z. Yin, D. Yang, T. Sun, H. Yu, H. E. Hoster, H. H. Hng, H. Zhang and Q. Yan, *Energy Environ. Sci.,* 2013, **6,** 987 – 993.

7 (**a**) R. Cai, H. Liu, W. Zhang, H. Tan, D. Yang, Y. Huang, H. H. Hng, T. M. Lim and Q. Yan, *Small*, 2013, **9,** 1036-1041. (**b**) L. Luo, J. Wu, J. Luo, J. Huang and V. P. Dravid, *Sci. Rep.,* 2014, **4,** 3863. (**c**) J. Luo, X. Zhao, J. Wu, H. D. Jang, H. H. Kung and J. Huang, *J. Phys. Chem.* Lett.*,* 2012, **3,** 1824-1829.

8 (**a**) J. H. Zhu, J. Jiang, W. Ai, Z. X. Fan, X. T. Huang, H. Zhang and T. Yu, *Nanoscale*, 2014, **6,** 12990-13000. (**b**) W. Ai, Z. M. Luo, J. Jiang, J. H. Zhu, Z. Z. Du, Z. X. Fan, L. H. Xie, H. Zhang, W. Huang and T. Yu, *Adv. Mater.* 2014, **26,** 6186-6192. (**c**) C. Guan, X. H. Wang, Q. Zhang, Z. X. Fan, H. Zhang and H. J. Fan, *Nano Lett.* 2014, **14,** 4852–4858.

9 (**a**) H. Yu, C. Guan, X. H. Rui, B. Ouyang, B. L. Yadian, Y. Z. Huang, H. Zhang, H. E. Hoster, H. J. Fan and Q. Y. Yan, *Nanoscale* 2014, **6,** 10556-10561. (**b**) W. Ai, Z. Z. Du, Z. X. Fan, J. Jiang, Y. L. Wang, H. Zhang, L. H. Xie, W. Huang and T. Yu, *Carbon,* 2014, **76,** 148-154. (**c**) D. Yang, Z. Y. Lu, X. H. Rui, X. Huang, H. Li, J. X. Zhu, W. Y. Zhang, Y. M. Lam, H. H. Hng, H. Zhang and Q. Y. Yan, *Angew. Chem. Int. Ed.,* 2014, **53,** 9352–9355.

10 (**a**) J. Jiang, J. H. Zhu, W. Ai, Z. X. Fan, X. N. Shen, C. J. Zou, J. P. Liu, H. Zhang and T. Yu, *Energy Environ. Sci.,* 2014, **7,** 2670-2679. (**b**) C. R. Zhu, X. H. Xia, J. L. Liu, Z. X. Fan, D. L. Chao, H. Zhang and H. J. Fan, *Nano Energy,* 2014, **4,** 105-112. (**c**) C. Guan, Z. Y. Zeng, X. L. Li, X. H. Cao, Y. Fan, X. H. Xia, G. X. Pan, H. Zhang and H. J. Fan, *Small,* 2014, **10,** 300-307.

11 P. G. Bruce, S. A. Freunberger, L. J. Hardwick and J.-M. Tarascon, *Nat. Mater.,* 2012, **11,** 19.

12 Y.Yang, M. T. McDowell, A. Jackson, J. J.Cha, S. S.Hong and Y. Cui, *Nano Lett.*, 2010, **10**, 1486.

13 J. M. Tarascon and M.Armand, *Nature*, 2001, **414** 359.

14 Y. Yang, G. Zheng and Y. Cui, *Chem. Soc. Rev.,* 2013, **42,** 3018-3032.

15 J. Xiulei and L. F. Nazar, *J. Mater. Chem.,* 2010, **20,** 9821.

16 R. D.Rauh, K. M. Abraham and G. F. Pearson, *J. Electrochem. Soc.,* 1979, **126,** 523-527.

17 J. Shim, K. A.Striebel and E. J.Cairns, *J. Electrochem. Soc.* 2002, **149,** A1321-A1325.

18 K. Kang, Y. S. Meng, J. Bréger, C. P. Grey and G. Ceder, *Science*, 2006, **311,** 977-980.

19 E. Peled and H.Yamin, *Prog. Batteries Sol. Cells*, 1984, **5,** 56-58.

20 R. D. Rauh, F. S.Shuker, J. M. Marston and S. B. Brummer, *J. Inorg. Nucl. Chem.,* 1977, **39,** 1761-1766.

21 S.-E. Cheon, et al. *J. Electrochem. Soc.,* 2003, **150**, A800-A805.

22 X. L.Ji, K. T.Lee and L. F. Nazar, *Nat. Mater.,* 2009, **8,** 500.

23 J. Schuster, G. He, B. Mandlmeier, T. Yim, K. T. Lee, T. Bein and L. F. Nazar, *Angew. Chem., Int. Ed.*, 2012, **51,** 3591.

24 N. Jayaprakash, J. Shen, S. S. Moganty, A. Corona and L. A. Archer, *Angew. Chem., Int. Ed.*, 2011, **123,** 6026.

25 J. Kim, D.-J. Lee, H.-G. Jung, Y.-K. Sun, J. Hassoun and B. Scrosati, *Adv. Funct. Mater.*, 2013, **23,** 1076-1080.

26 G. Zheng, Y. Yang, J. J. Cha, S. S. Hong and Y. Cui, *Nano Lett.,* 2011, **11,** 4462.

27 J. Guo, Y. Xu and C. Wang, *Nano Lett.* 2011, *11*, 4288.

28 R. Elazari, G. Salitra, A. Garsuch, A. Panchenko and D. Aurbach, *Adv. Mater.* 2011, **23,** 5641.

29 L. Ji, M. Rao, H. Zheng, L. Zhang, Y. Li, W. Duan, J. Guo, E. J. Cairns and Y. Zhang, *J. Am. Chem. Soc.*, 2011, **133,** 18522.

30 H.Wang, Y. Yang, Y. Liang, J. T. Robinson, Y. Li, A. Jackson, Y. Cui and H. Dai, *Nano Lett.,* 2011, **11,** 2644.

31 X. Ji, S. Evers, R. Black and L. F. Nazar, *Nat. Commun.,* 2011, **2,** 325.

32 S. Evers, T. Yim and L. F. Nazar, *J. Phys. Chem. C*, 2012, **116,** 19653.

33 R. Demir-Cakan, M. Morcrette, F. Nouar, C. Davoisne, T. Devic, D. Gonbeau, R. Dominko, C. Serre, G. Feryey and J.-M. Tarascon, *J. Am. Chem. Soc.*, 2011, **133**, 16154.

34 Y. Fu, Y.-S. Su and A. Manthiram, *ACS Appl. Mater. Interfaces*, 2012, **4,** 6046.

35 V. C. Tung, M. J. Allen, Y. Yang and R. B. Kaner, *Nature Nanotech.,* 2009, **4,** 25-29.

36 L. H. Hu, F.Y. Wu, C. T. Lin, A. N. Khlobystov and L. J. Li, *Nat. Commun.*, 2013, **4**, 1687.

37 D. W. Wang, F. Li, M. Liu, G. Q. Lu and H. M. Cheng, *Angew. Chem. Int. Ed.,* 2008, **47,** 373–376.

38 C. Y. Su, A.Y. Lu, Y. Xu, F-R. Chen, A. Khlobystov and L. J. Li, *ACS Nano,* 2011, **5,** 2332.

39 **(a)** Z.-K. Wei, J.-J.Chen, L.-L.Qin, A.-W.Nemage, M.-S.Zheng and Q.-F. Dong, *J. Electrochem. Soc.* 2012, **159,** A1236, (**b**) Y. Zhao, J. Feng, X. Liu, F. Wang, L. Wang, C. Shi, L. Huang, X. Feng, X. Chen, L. Xu, M. Yan, Q. Zhang, X. Bai, H. Wu and L. Mai, *Nat. Commun.,* 2014, **5**, 4565.

40 X. L. Ji and L. F. Nazar, *J. Mater. Chem.* 2010, **20,** 9821.

41 S. Chen, X. Huang, B. Sun, J. Zhang, H. Liu and G. Wang, *J. Mater. Chem. A*, 2014, **2,** 16199.

42 Y.-X. Wang, L Huang, L.-C. Sun, S.-Y. Xie, G.-L. Xu, S.-R. Chen, Y.-F. Xu, J.-T. Li, S.-L. Chou, S.-X. Dou and S.-G. Sun, *J. Mater. Chem.* 2012, **22,** 4744.

43 S. S. Zhang, *J. Power Sources*, 2013, **231,** 153-162.